LA-UR-22-20012

Approved for public release; distribution is unlimited.

Title:	Intentional Uranium Tagging for Material Provenance and Pathway Forensics (LA19-Intentional-Forensics-NDD3Bb): Final Project Report
Author(s):	Hackenberg, Robert Errol; Black, Amber Nalani; Bloom, Rose Anne; Carpenter, John S.; Cooley, Jason Christopher; Imhoff, Seth D.; Luitjohan, Kara Eileen; Luther, Erik Paul; Montgomery, Colt James; O'Brien, Lindsay Beth; Stull, Jamie Ann; Tegtmeier, Eric Lee; Winter, William Paul III
Intended for:	Report
Issued:	2022-01-03

Intentional Uranium Tagging for Material Provenance and Pathway Forensics (LA19-Intentional-Forensics-NDD3Bb): **Final Project Report**

Robert E. Hackenberg, Amber N. Black, Rose A. Bloom, John S. Carpenter, Jason C. Cooley, Seth D. Imhoff, Kara E. Luitjohan, Erik P. Luther, Colt J. Montgomery, Lindsay B. O'Brien, Jamie A. Stull, Eric L. Tegtmeier, William P. Winter III

Sigma Manufacturing Sciences Division
Los Alamos National Laboratory

written in December 2021

LA-UR-

ABSTRACT

This report summarizes the outcomes of a 3-year NA-22 exploratory project to research the feasibility of tagging uranium materials, especially nuclear fuels, for nuclear nonproliferation purposes. The experimental focus was on metallic uranium forms under prospective surface and bulk tagging manufacturing and detection scenarios. This study showed that a large number of tags (drawn from an even larger menu of options) could be successfully imparted and detected in both as-built and degraded conditions. These results pave the way for additional R&D studies of surface and bulk tagging of metallic forms of uranium.

Multiple surface tagging techniques and detection strategies were explored with an emphasis on tag quality, readability, and detection in the field. Non-radioactive materials were used as a testbed. Selective deposition via laser beam was successful in imparting readable titanium deposits on a stainless steel base plate. These tags were read with both high resolution characterization techniques (e.g., scanning electron microscopy) and field-capable tools (e.g., eddy current testing, handheld x-ray fluorescence). These field-capable tools were basic, off-the-shelf models, but improvements in detection can be gained from the use of more high-end instrumentation in follow-on work. A literature review of photoluminescence was carried out as an exploration of an unconventional surface tagging strategy, and various manufacturing strategies assessed. These initial results were encouraging, and the opportunity space for various tag design, manufacturing and detection approaches remains large.

To survey bulk taggant elements for bulk uranium metal, 16 tagging elements (among a possible 43 pre-screened elements) were experimentally examined. A total of 18 depleted uranium castings were made and their tagging signatures characterized. Elemental concentrations of 0.5 wt.% or lower were used to demonstrate the making and measuring of the tags, with the intention of still lower concentrations in plausible nuclear fuel tagging scenarios. A common alloying-melting-casting manufacturing method allowed two detection options for all

tagging elements: bulk chemical analysis (for “chemical taggants”) and microstructural analysis (for “second phase taggants”). Taggant acceptability was based upon manufacturability, detectability, chemical homogeneity, and persistence from the standpoint of both up-front manufacturing and in the face of “degradations” such as dilution, mixing, and recycling. Manufacturability was generally good: apart from one anomalous casting at project start, the elements of interest made it into their respective castings, and very encouragingly, without any preferential segregation to the top or bottom of the castings, meaning they were chemically homogeneous. Two independent laboratories carried out chemical analysis on most of the castings, with generally good agreement between the two labs. Scanning electron microscopy with energy dispersive spectroscopy microanalysis revealed the tagging elements mostly ended up in the anticipated second phases. The shapes and spatial distributions of these micron-sized carbides, oxides, and intermetallic particles offers opportunities for further science-based investigation and tagging optimization.

Overall, V and Co currently appear as the best choices for chemical taggants while Al, Ti, Mn, Co, Pd, and Tb all look good as second phase taggants. The other elements considered here – Sc, Ni, Ge, Nb, Ce, Ta, W, Ir, and Au – while not being ruled out, require more study to become viable options. It is of special note that in the recycling study only one of the 12 elements fell out of detection even after 10 meltings, demonstrating their persistence.

Although not all of the ideas were successful or even tried, the data from these preliminary trials paves the way for follow-on work. On the materials science and manufacturing side, more research is needed to explore, for example, luminescence (surface), the remaining 27 pre-screened elements that were not studied (bulk), and more fundamental mechanisms of alloying during melting and solidification (surface and bulk). On the detection side, wider ranges of tagging intensity (e.g., depth of penetration surface deposits; bulk tagging element concentrations) can be probed and more statistical testing should be done. Overall, this work demonstrated proof of concept for a broad range of surface and bulk tagging options.

CONTENTS

LIST OF ACRONYMS AND SYMBOLS

BCC	body-centered cubic
BSE	back-scattered electron
CNO	carbide and/or nitride and/or oxide
DU	depleted uranium (<0.7% U-235, typically 0.2%)
EB	electron beam
EBSD	electron backscatter diffraction
EC	eddy current
EDM	electrical discharge machine
EDS	energy dispersive spectroscopy
HT	hot top
ICP-MS	inductively coupled plasma-mass spectrometry
LANL	Los Alamos National Laboratory
LEU	low-enriched uranium (<20% U-235)
LOM	(visible) light optical microscopy
LWR	light water reactor
NDT	non-destructive testing
PEO	plasma electrolytic oxidation
PFIB	plasma focused ion beam
SE	secondary electron
SEM	scanning electron microscope
SNM	special nuclear material
Tb	boiling point or element terbium
TEM	transmission electron microscope
Tm	melting point
TRL	technology readiness level
XRF	x-ray fluorescence
VIM	vacuum induction melt
wppm	weight parts-per-million
wt.%	weight percent
X	generic element
Z	atomic number

1. INTRODUCTION

1.1. Mission relevance, goals and impact

This project was initiated in FY19 in response to the proposal call issued in fall 2017 under the Nuclear Forensics Program the U.S. Department of Energy Office of Nonproliferation Research & Development (NA-22).

This exploratory project examines strategies for encoding unique signatures into uranium at its manufacturing source. The proactive tagging approach enables discriminating forensics information to be extracted should the material be lost and later interdicted. Deliberate upstream tagging at the originating entity for (future) uranium streams provides provenance, while additional, co-located observables in the material can give clues as to the attributes of both pathway and perpetrator, in the sense of revealing any additional processing the material experienced (e.g., bulk melting or welding) before interdiction or recovery of regulatory control.

This project initially set out to explore and extend the possibilities of multiple tagging strategies, including:

1. **Surface Tagging** by inscribing unique patterns on uranium metal surfaces,
2. **Bulk tagging** by altering the bulk chemistry of **metallic forms** of uranium via microalloying, and
3. **Bulk tagging** by altering the bulk chemistry of **uranium dioxide**.

If successful, this work will continue the technical maturation process of these taggant technologies to reach a later point where they could be incorporated into industrial-scale uranium manufacturing and potentially, reprocessing streams as well. It can likewise affect next-generation international agreements.

More broadly, this enables a proactive forensics capability that intentionally controls its circumstances to reshape the playing field to our advantage, with improvements in reliability and robustness anticipated over the longer term. By fingerprinting uranium, it can be known far better than before just where the material originated, which narrows the search to viable suspects, sites, and materials streams while at the same time possibly ruling out the majority of unimplicated entities.

Figure 1.1 provides a wider context for tagging vis-a-vis the nuclear fuel cycle. The experimental portion of this work was focused on imparting the tag – whether surface (step G) or bulk (step F) – and detecting it in nominal and degraded conditions.

The spirit of this project was the initial exploration of possibilities, not a deeper dive into one or two focused end-to-end nonproliferation scenarios. End-use considerations informed but did not unduly limit our explorations. Obvious show-stoppers were recognized and avoided, but more detailed case studies of the manufacturability, vendor acceptance, and in-reactor performance, as important as they are, were beyond the scope of this project.

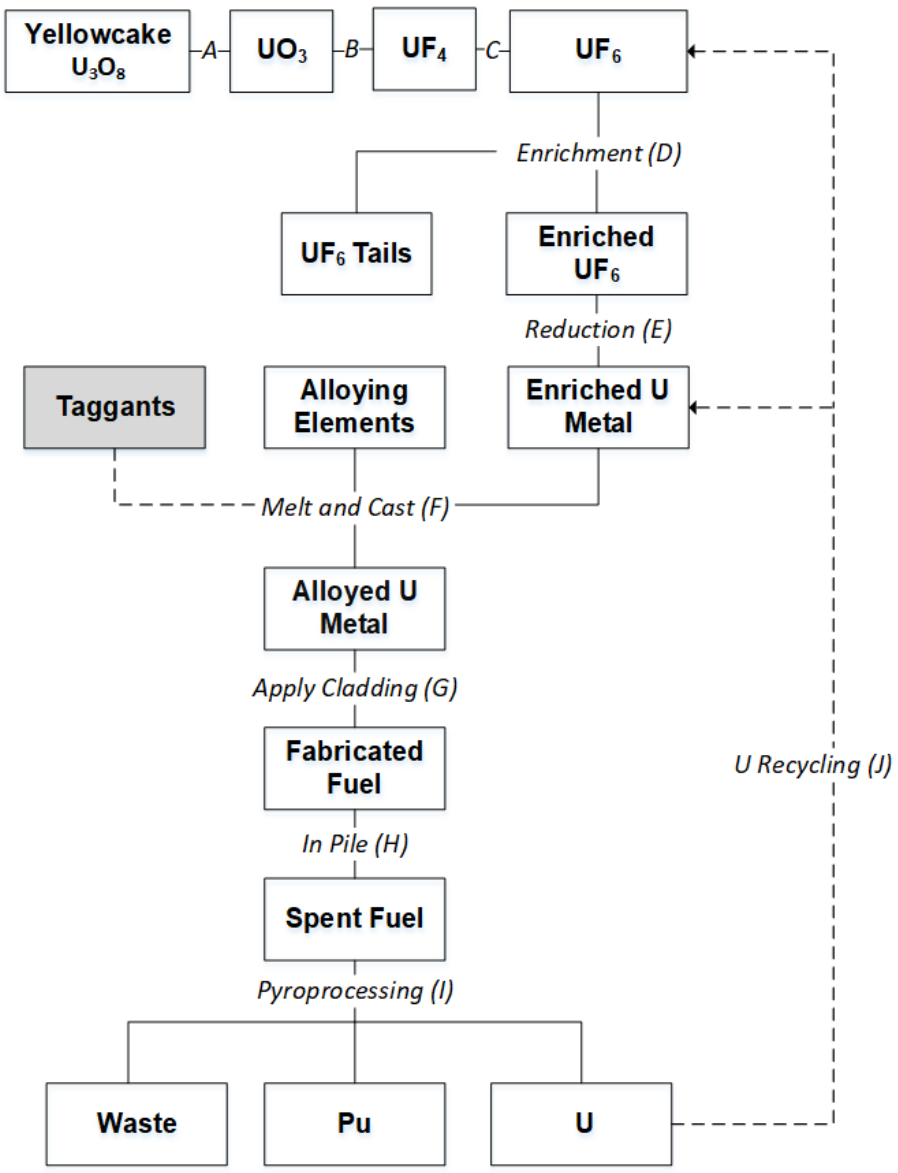

Figure 1.1. Flowchart of the metallic fuel lifecycle from ore through spent fuel reprocessing and recycling. This figure is specific to bulk tagging; flow is similar for surface tagging, where the tagging insertion can be before or after the cladding step (G).

1.2. Overview of project activities and structure of this report

For prior work and a broad survey of tagging strategies that were initially considered, see the FY19 report for this project [2019hac]. New and updated experimental results and some paper studies are in the FY20 and FY21 reports [2020hac, 2021hac].

A survey and downselect of tagging elements and tagging strategies in FY19 resulted in these preliminary conclusions, which informed the course of the project:

1. Tags will not survive fluorination, defluorination, and isotopic enrichment steps; they are only marginally likely to survive reprocessing steps (see Figure 1.1).
2. Headspace exists in all uranium-based nuclear fuels for bulk tagging chemical additions. The headspace is very much element-dependent.
3. The uniqueness of bulk tagging with regular elements lies in the ratios among a suite of elements; the default detection scheme is traditional chemical analysis.
4. Bulk taggants are best added at the step when oxide, nitride, or silicide powders are blended before pellet pressing, or when metallic uranium is melted and cast.
5. Surface tagging is also viable, admits of a wider array of options (few of them well-developed), and is more amenable to stand-off and nondestructive detection.

Owing to resource limitations, strategy #3 (Section 1.1), bulk tagging of uranium dioxide was not pursued beyond initial discussions and a paper study outlining the major issues that was documented in FY20 [2020hac]. The remaining two strategies, surface tagging and bulk tagging (both on uranium metal), were run through to a reasonable completion in these three years, and in spite of the Covid-19 pandemic starting in March 2020, just 6 months after project start.

The following sections summarize surface tagging (Section 2) and bulk tagging (Section 3). Recommendations for follow-on work are given. **Shorter summaries are in 2.1 and 3.1.**

2. SURFACE TAGGING

2.1. Overview and summary

Deposition of titanium on either titanium or stainless steel using electron-beam (EB) and laser methods was studied for all 3 years of the project. Figure 2.1 shows a successful deposit. A variety of detection methods were explored. In some cases the as-built tag was deliberately degraded, e.g., by abrasion, to test detectability in such situations. Details are in Section 2.2.

A paper study of luminescence options for tagging was issued in FY21 [2021blo] and is summarized in Section 2.3.

The overall outcomes of surface tagging in this project are summarized in the stoplight chart, Table 2.1.

Figure 2.1. John Hancock and Ben Franklin signatures produced with laser selective deposition (60 and 35 mm long, respectively). An EOS M290 additive manufacturing machine was used. The deposition was produced with 0.015 mm pure Ti foil on a 316L stainless steel plate.

Table 2.1. Summary of surface tagging and detection strategies evaluated as part of this project. Relative success is shown for each item. Red indicates an item that was determined to be not successful, is not viable, or is not a path worth considering when compared to other options. Yellow indicates an item that is feasible, but additional work is necessary to prove success for surface tagging. Green indicates an item that demonstrated initial success as part of this project, and is the most promising candidate for further exploration.

	Manufacture or Detection Method	Summary (Surface Tagging)	
Deposition Technique	Electron Beam Deposition with Wire		Utilizing an older EB system, the wire deposition was too large for surface applications, and limited in potential designs (i.e., only a straight line was possible). This is due to the wire size and low voltage of the system.
	Electron Beam Deposition with Ti Foil		Utilizing a newer EB system and titanium foil (rather than wire), signatures were attempted in similar detail to the laser deposition. Titanium deposition was not successful, primarily due to the charged nature of the electron beam. Further exploration into securing the foil to the base plate may show success, but was not attempted due to success with laser beam deposition.
	Laser Beam Deposition with Ti Foil		Utilizing an additive manufacturing system (EOS M290), selective laser deposition was able to create intricate Ti-deposited signatures (John Hancock and Ben Franklin replicas) on SS 304L and 316L base plates.
	Laser Beam Deposition with Ti Foil, Improved Beam Parameters		Improvements on the successes using laser beam depositions from FY19 and 20 were attempted in FY21. Slowing the laser beam speed, and/or increasing the power of the beam, showed improvements in deposition by way of an increase in deposited titanium across the length of the signature, and homogeneity in the solidified melt pool between the titanium and the stainless steel base plate.
	Plasma Focused Ion Beam		Attempts at depositing very small signatures using platinum were not successful; deposition was not detected using X-ray fluorescence (XRF) or eddy current.
Detection Technique	Electron Microscopy: BSE, EDS		Imaging using backscatter electrons (BSE) and energy dispersive X-ray spectroscopy (EDS) was successfully used to detect titanium in the plan and cross-section views. Improvements in laser beam deposition made detection in the plan view easier in FY21 compared to FY20. These techniques do require a scanning electron microscope, but are easy for a trained user.
	Electron Microscopy: EBSD		Electron backscatter diffraction (EBSD), although useful for grain size investigation, was not pertinent to this project as a standalone microscopy tool, and requires additional skill and training for an operator to generate.
	XRF		XRF was utilized as a field-ready technique to determine the presence and quantity of titanium in a signature. Although useful for detecting titanium quickly, results showed bias due to remnant (unmelted) titanium that was left behind after deposition, and there was no feasible way to detect a spatially varying signature, as the measurement is taken from a large surface area.
	Eddy Current		Eddy current showed significant success in detection of titanium, even after the signature had been partially removed by hand via sandpaper. Although not demonstrated due to the eddy current system available, spatial detection of titanium (i.e., detection of a pattern) is possible with available eddy current systems on the market.
	Photo-luminescence		A literature review [2021blo] showed a variety of potential luminescent tags exist. Although some are likely impractical for use in a nuclear reactor environment, due to environmental degradation of the tag, compatibility with the fuel, degradation of reactor performance, etc., several strategies were identified as potentially viable candidates for nuclear fuel tagging.

2.2. Experimental studies

This project focused on depositing or altering the surface of a material by localized melting. To avoid radioactive materials during process development, titanium was deposited on base plates of 304L or 316L stainless steels. “John Hancock” and “Ben Franklin” signatures were imparted using a laser-based EOS M290 machine (Figure 2.1), as were other patterns such as Braille characters. Laser methods proved more versatile than EB methods, and they improved over time (Figure 2.3) and could benefit from even further studies. EB methods did improve over the course of the project (including the use of foil instead of wire) and should not necessarily be ruled out, although they are clearly a second choice with respect to laser methods.

Detection was attempted using scanning electron microscopy (SEM) with 4 imaging/mapping modes:

- standard secondary electron imaging (SE),
- backscatter electron imaging (BSE),
- energy dispersive spectroscopy (EDS), and
- electron backscatter diffraction (EBSD) for grain orientation mapping and texture.

These SEM-based characterization methods are the most labor-intensive of these detection methods considered in this work but gives the most information. In addition, simpler field-ready tools such as x-ray fluorescence (XRF), and eddy current (EC) were also explored and will be remarked upon.

The deposited patterns (Figure 2.1) can be clearly seen in plan view by regular SE imaging in an SEM, but backscatter electron imaging (BSE) could also reveal the Ti distribution (Figure 2.2). EDS is the ideal method in principle as it directly yields maps of local material compositions. EDS done in plan view (the easiest orientation to work with, as it involves no or little specimen preparation) gave marginal results (not shown here) for the patterns, though it could improve with more uniform melting of the Ti. As expected, EDS done in the more labor-intensive cross-sectional view (Figure 2.3) showed the Ti melted into the SS base plate.

One might ask how an SEM could spatially locate deposition signatures in an unknown specimen where the overall specimen dimensions might be larger and the surface tag considerably smaller and more subtle. Emerging SEM software algorithms can meet this challenge. AztecLive, a rapid-detection software option available with Oxford Instruments EDS detectors, was used for quick detection of titanium in the plan view images shown in Figure 2.3. This tool allowed for quick determination of locations where titanium was present, which are then further evaluated by the user to gather higher resolution images and data.

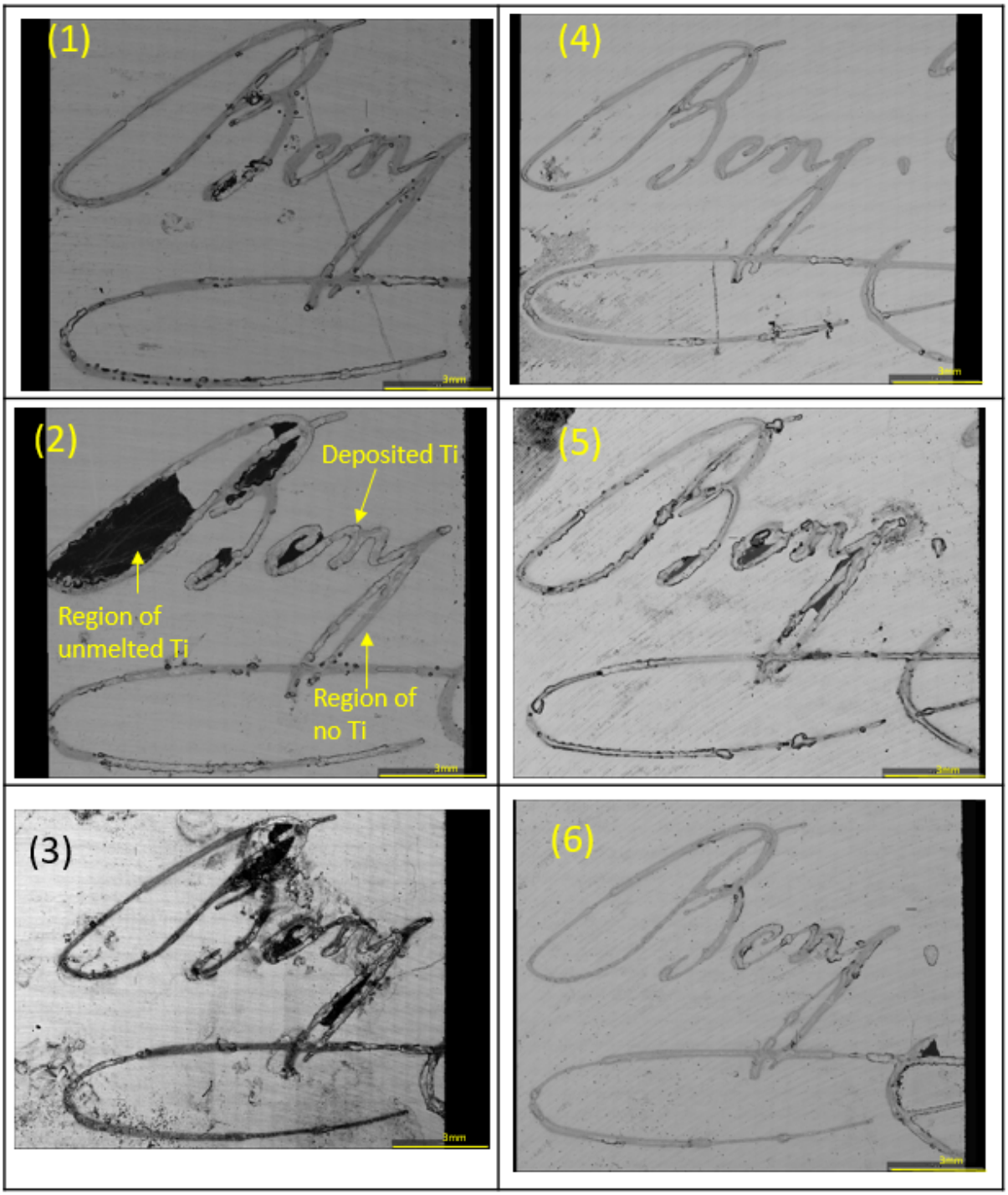

Figure 2.2. SEM images of "Ben" signature from 6 different laser deposition runs of Ti foil on 304L stainless steel. Signature 2 is used to demonstrate the appearance of regions with titanium or no titanium, as a way of assessing quality of tag manufacture. The deposited Ti in the form of the signature was the intended tag; regions of un-melted Ti were not desired. Backscatter electron imaging mode was used (not to be confused with EBSD grain mapping.)

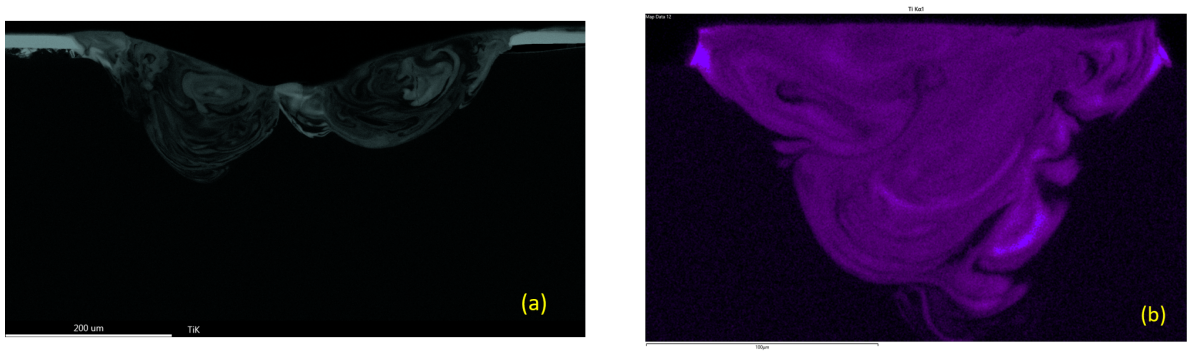

Figure 2.3. SEM-EDS cross-section maps of laser titanium signature deposits from (a) FY20 baseline parameters (on 316L) compared to (b) FY21 signature 5 (on 304L; increased laser power). Brighter indicates increased Ti concentration. Adjustments have been made to both images to improve brightness and contrast. Note that the (b) FY21 signature is taken at a higher magnification compared to the (a) signature from FY20; the scale bars read: (a) 200 micron (b) 100 micron. Although both parameter sets have deposited titanium, the increase in laser power improves the distribution of titanium in the cross-section of the signature as evidenced by increased homogeneity with respect to brightness level in map b.

EBSD revealed the grain structure in the melted and neighboring areas in cross-section (again, needing relatively labor intensive specimen preparation). This by itself did not reveal much information relevant to tagging quality; EDS was determined to be the method of choice, and EBSD is recommended only where one needs to know the grain structure to assess welds or other localized melting.

Handheld XRF is a potential stand-off method and it detected the Ti at measurable but low levels on the surface (1-10 wt.%, as opposed to a 100% theoretical limit). The instrument used in this work has limited spatial resolution that restricts its applicability to unknown samples or finer-scale features. More advanced XRF instruments that are more amenable to 2D mapping should be considered in future work. Replicability studies would also be needed to confirm that readings are the result of deposited Ti (as opposed to instrument or background uncertainties).

Finally, point-probe eddy current (EC) was able to detect a difference between areas that had Ti melted into the base plate vs. areas where no Ti was deposited, even if the base plate was melted in the same pattern. Although EC only gives qualitative results on what elements were tagged (right now a yes/no-type answer), more advanced EC instruments have the potential to detect 2D patterns where identifying specific tagging elements is unimportant, such as braille or QR codes, and should be explored further.

An initial effort to explore microscopic tagging of platinum (~0.25 mm squares x 2 micron thick) onto stainless steel was done in using a plasma focused ion beam (PFIB) but could not be detected by XRF or EC. (Detection by SEM-EDS was expected to work, though.) Given the low throughput of a PFIB, this precision deposition method is not recommended for the expected high-volume tagging applications.

Combinations of various surface tagging methods into a single pattern are certainly options but were not explored in this study. Such combinations can provide defense-in-depth and allow both destructive and nondestructive detection methods to be used.

2.3. Literature review of photoluminescence

Photoluminescence was proposed as a potential surface tagging strategy during one of the team's brainstorming sessions, and a literature review was done in FY21 to determine the feasibility of utilizing luminescent tags for this application. A full report was issued detailing several of the findings from this review [2021blo].

A variety of potential luminescent tags exist for surface tagging applications, including method of generating tag, material type or compound, and maturation of the technology. Dye, paint, thin films, thick films, and plasma electrolytic oxidation (PEO) coatings were all considered, and a stoplight chart was provided in the report summarizing their applicability and maturity. Uranium oxide is naturally luminescent, which confounds (or in some cases could potentially help) detection of tags in uranium fuel, whether metallic of oxide. Another promising route would be to utilize PEO coatings. This technique is being used for valve metal surfaces, and this list includes Zr, which is utilized (typically in the zirconium alloy form) in the nuclear industry for fuel cladding. Therefore, PEO coatings may be readily available as surface tagging methods for zircaloy cladding.

Taken as a whole, luminescence offers a promising route to stand-off detection of tags but is relatively immature for reactor fuel applications, so more study would be needed. Thin films on metallic uranium fuel or PEO coatings of cladding materials might be a good place to begin.

2.4. Recommendations for follow-on work

In no particular order, the following are logical next steps in advancing surface tagging.

2.4.1. Continuation of laser deposition and detection work

Laser deposition proved to be superior to the electron-beam deposition. Studies of titanium deposits on stainless steel (and perhaps other combinations of metals and alloys) should be continued to improve the process, explore smaller and more subtle signatures, and perform replicability trials with respect to microscopy and eddy current detection. Detection will continue by 2D eddy current (see below), SEM-EDS, and more advanced XRF instruments that are more amenable to 2D mapping.

2.4.2. Detection by eddy current mapping

The EC work in this study showed promising results (i.e., differences between Ti-altered and unaltered stainless steel). However, it was based on a simple point-probe instrument. A higher-end EC instrument would have the ability to map out EC signal in a 2D region, revealing spatially-encoded information such as the John Hancock / Ben Franklin, Braille, etc. signatures.

2.4.3. Incorporating surface taggants by localized melt pools on metal fuels

Localized melting through various welding technologies offers a controlled method to change the surface of a material. High energy density processes offer low heat inputs and shallow melt pools, which can affect a small volume of material on the surface. Due to the rapid solidification, certain features can be frozen or suspended in position, including inclusions/additives, alloy

elements, or even defects. Continued development of a foil method is suggested to begin with; other methods such as particulate additives that are fused into place will also be explored. These features can be non-obvious but detectable by the forensics community. This will offer a wider menu of options for surface tagging. Possible detection methods for the forensics community include eddy current, micro x-ray fluorescence, blacklight (for fluorescent taggant particles) and microscopy (SEM most likely, with light optical a possibility.) A particulate strategy offers a rare chance to study fundamentals of fluid flow in localized melting for surface tagging and for welding more broadly.

2.3.4. Plasma electrolytic oxidation (PEO) coatings of cladding

PEO Is a viable option for tagging-the-cladding with a luminescent material, as zirconium has been specifically explored due to its use as a valve material. Trial deposition of these tags (yet to be identified) on zirconium metal or zirconium-based alloys can be likely be performed at Sigma or possibly elsewhere.

3. BULK URANIUM METAL TAGGING

3.1. Overview and summary

Bulk tagging was done by adding selected elements to uranium. This section summarizes the outcomes for the 16 elements added to metallic uranium by melting and casting (of 43 elements deemed initially suitable). The following sections provide additional detail of element selection (3.2), experimental methods (3.3), and alloy manufacture and characterization (3.4).

This task focuses on **chemical tagging** – adding various elements in specific ratios to provide a unique taggant signature in bulk metal uranium. Ideally, the ratios of the taggant elements will remain the same even with dilution through further material processing. This strategy is detectable through bulk chemical analysis such as inductively coupled plasma-mass spectroscopy (ICP-MS).

A different strategy – **second-phase tagging** – also arises since the formation of second phases is likely to occur when alloying elements are added to a metal. Each element will preferentially distribute to various phases (carbides, oxides, nitrides, intermetallics, and/or the uranium-rich matrix) according to the phase diagram. Elements that normally are hard to detect by chemical analysis can be found in these particles with high local concentrations. Scanning electron microscopy (SEM) and energy-dispersive X-ray spectroscopy (EDS) were used to detect these signatures.

The potential taggants were probed for detectability and behavior in three distinct stages of experimentation. The elemental additions were first alloyed with uranium at relatively high concentration levels (0.5 wt.%) in unique groupings of four elements in order to probe initial detectability. These are the baseline castings, and have about 98 wt.% uranium by difference.

Taggant persistence in the face of degraded conditions was then examined. Further mixing and dilution castings were performed in order to observe both species interaction as well as detectability. Finally, a recycling study was used in order to determine the persistence of the alloying additions after repeated melting and casting of the same material. A variety of microscopy and chemical assessment techniques were utilized to track the fate of the taggant element additions.

In total, 18 castings were made and analyzed in this project: 4 baseline, 3 mixed, 1 dilution, and 10 recycled, which gave a reasonably comprehensive first take on the suitability of various elements as bulk taggants. ***The overall outcomes of bulk tagging of the 16 elements examined in this project are summarized in the stoplight chart, Table 3.1.*** Specific element-by-element details appear in the text following the table.

Later on in the project, a paper study was also conducted to examine codes and specifications of fuel forms, reactor types, and cross-sections of the 16 elements under consideration. A brief review was performed to understand if these elements had any unique nuclear characteristics (cross-sections) that would interfere with the performance of the reactor, are known to be used in reactors, or if any fission or activation products were known to be an issue. See the FY20 report [2020hac] for details, including an element-by-element chart of the 16 elements of interest. This in-depth examination was done about halfway into the project, so some of the insights (e.g., the unattractively high thermal absorption cross-section of iridium) did not factor into the selection of the bulk tagging matrix of 16 elements.

Table 3.1. Stoplight chart summarizing how each element would behave as either a chemical taggant or second phase taggant based on the current set of results. The outcome is based on manufacturability and detectability in both nominal (baseline) and degraded conditions.

Element		Bulk tagging strategy	
Name	**Symbol**	**Chemical taggant**	**Second phase taggant**
Aluminum	Al		
Scandium	Sc		
Titanium	Ti		
Vanadium	V		
Manganese	Mn		
Cobalt	Co		
Nickel	Ni		
Germanium	Ge		
Niobium	Nb		
Palladium	Pd		
Cerium	Ce		
Terbium	Tb		
Tantalum	Ta		
Tungsten	W		
Iridium	Ir		
Gold	Au		

Good choice
More work is needed
Should not be pursued without a lot more study
Downscoped from project due to processing issues

An element-by-element survey of the **suitability for chemical tagging** now follows. The "previous study" is referenced in [2013hac] (and the annual reports FY09-FY12 it cites which led to this final report in 2013.) The only metals chemical analyses in that study were from the two

VIM castings of the same composition that contained (nominally) 0.05 wt.% each of Ti, V, and Mn, and 0.10 wt.% each of Zr, Mo, and Au.

Two elements showed the **best results** (green in Table 3.6):

- V and Co
    - Detectable by two different laboratories.
    - Measured at their expected values after proper mixing during processing.
    - Remained at a consistent level through 10 casting cycles.
    - Good V result consistent with previous study.

Six elements, appearing as yellow in Table 3.5, showed **fair results** (yellow in Table 3.6) and need to be further studied before a decision should be made. The issues for these are:

- Al and Ti
    - Did not measure at their expected values.
    - Low Ti result is consistent with previous study.
    - Noticeable difference between the different locations per casting throughout the recycling study.
- Pd and Au
    - Unexplained trends in measured chemistry in the recycling study.
    - Au showed a good result (measured at or somewhat above nominal) in previous study.
- Nb
    - Measured lower than expected in the recycling study.
    - Measured at its expected value in the mixed/dilution castings.
- Mn
    - Could have slightly decreased over the course of ten castings, but to determine if this trend is real, more castings would need to be carried out.
    - Showed a good result (measured at nominal) in previous study.

Four elements (all red) showed the **poor results** (red in Table 3.6). Without a good deal more study, these should not be considered for chemical taggants

- Sc and Tb
    - Measured much lower than their calculated values.
        - Could be a detection issue with ICP-MS.
        - Could be a processing issue since these elements can be difficult to incorporate into uranium.
- W and Ir
    - Two laboratories did not agree on the measured values.

It is of special note that in the recycling study only 1 of these 12 elements fell out of detection (Tb, which began at a very low level to begin with) even after 10 meltings, demonstrating their persistence.

Finally, four elements – Ni, Ge, Ce, Ta – are **inconclusive** (gray in Table 3.6), as their baseline casting had issues with a visible reaction in the crucible. It should be noted that in the previous NA-22 study [2013hac], all four of these elements were included in arc melted alloys, but resource limitations prevented their chemical analysis (apart from C, N, O analyses). Having

said that, TEM was able to identify phases containing Ni, Ce, and Ta; Ge was not identified (intermetallics were expected) but that does not rule out its possible incorporation into alpha-uranium matrix or other second phases. So this indicates at least some amount of Ni, Ce, and Ta made it into the materials and could be suitable for chemical tags.

For **suitability for second-phase tagging**, six elements – Al, Ti, Mn, Co, Pd, and Tb – were able to be located in their expected phases via SEM-EDS and are considered good options for this tagging strategy. Five elements, Sc, V, Nb, Ir, and Au, were not always found in their anticipated second phase. These elements could still be viable second phase taggants as long as the alloy is fully and carefully characterized. Only one element, W, was not located in any of the alloys, and is therefore should not be pursued as a second phase taggant. And as mentioned in the preceding paragraph, Ni, Ge, Ce, and Ta were not further studied in this work, though the previous study found Ni, Ce, and Ta in second phase particles by TEM, demonstrating their suitability as second-phase tags.

3.2. Background – tagging element screening and selection

Given that the ratios of the taggant elements, not their absolute quantities, are relevant for tagging identification, a significant number of alloy elements were employed to increase the number of elemental ratios that can be exploited. This recognizes that not all the elemental pairings will be useful for accurate, discriminatory ratio identification after significant dilution and recycle, for example, due to chemical analysis limitations.

A matrix of four baseline alloys with four taggant elements each was a reasonable compromise between maximizing the number of elements – 16 in all – while avoiding excessive complexity in the chemical interactions during melting, solidification, and solid-solid phase changes.

The entire Periodic Table of the Elements up to Z=96 was initially considered and each element was screened for practical suitability through three filters that reduced the total number from 96 to 65 to 43. The first two filters were repeated from the prior NA-22 project.

The first filter removed 31 elements that were too common, a noble gas, especially rare, very reactive, acutely hazardous and/or administratively difficult – namely: H, He, Be, C, N, O, F, Ne, Cl, Ar, Br, Kr, Rb, Tc, Sb, I, Xe, Cs, Pm, Hg, Po, At, Rn, Fr, Ra, Ac, U, Np, Pu, Am, and Cm.

The second filter involved a more graded approach. The 65 elements surviving the first filtering step were then assigned negative points for:

- low boiling points Tb (e.g., Mg, Te, Cd, Eu, Bi),
- high melting points Tm (e.g., Mo, Hf, W),
- liquid immiscibility (e.g., Cu), and
- known chemical analysis difficulties (e.g., Si, P, K, Ca, Cr).

Elements having 0, 1, 2, or 3 of these negative points were graded, respectively, as “A” (most suitable), “B”, “C”, and “D” (least suitable). In the second filter, the 17 elements graded as “C” or “D” were excluded from any further consideration, reducing the total to 48 elements.

Then in the third and final filter, a subset of five “A” and “B” elements (B, Si, Mo, Gd, Dy) having poor neutronic or other characteristics pertinent to candidate metallic (LEU-Mo) or intermetallic (U-Si) fuels were also excluded.

Table 3.2 shows the 43 remaining elements that survived all three filters and were considered suitable as prospective taggants. In principle all these elements could have been examined. However, time and resource constraints resulted in a further downselection to 16 of them for this study. These 16 were picked based upon immediate availability of the elements and to provide a balance of various predicted second phases that might form. We desired more than one type of phase in each alloy, for example, at least one CNO-forming (carbide-nitride-oxide) element and one intermetallic-forming element in each casting.

The 16 elements examined in this study, and the 12 elements from the FY09-FY12 study [2013hac] are also noted in the far right column of Table 3.2. This table allows one to quickly identify the other 27 elements that were not studied here but are metallurgically viable. Table 3.3 lists the elements and the prediction of which phase they would end up in.

Table 3.2. Prescreened elements considered desirable for bulk tagging of uranium metal (43 total). The two right-side columns show the application of specific elements from the baseline alloys in this study as well as all materials in the previous NA-22 study. Time and resource constraints prevented all 43 element from being examined; those that were examined in this and the previous [2013hac] study are listed in the columns on the right side with their casting identification number or label.

Symbol	Z	Tm (C)	Tb (C)	Filter 2 negative Characteristics					Filter 2 grading	Castings made	
				Tm 0: <2000C -1: >2000C	Tb 0: >2000C -1: 1135-2000C -2: <1135C	Liquid immisc. 0: no -1: yes	Chemical analysis 0: ok -1: difficult	Sum		in this study	in the previous study
Al	13	660	2520	0	0	0	0	0	A	19C1-014	
Sc	21	1541	2831	0	0	(1)	0	(1)	B	19C1-014	
Ti	22	1670	3289	0	0	0	0	0	A	19C1-010	VIM#1
V	23	1910	3409	0	0	0	0	0	A	19C1-014	VIM#1
Cr	24	1863	2672	0	0	0	(1)	(1)	B		
Mn	25	1246	2062	0	0	0	0	0	A	19C1-010	VIM#1
Fe	26	1538	2862	0	0	0	0	0	A		
Co	27	1495	2928	0	0	0	0	0	A	19C1-015	
Ni	28	1455	2914	0	0	0	0	0	A	19C1-016	AM#2
Cu	29	1085	2563	0	0	(1)	0	(1)	B		
Ga	31	30	2205	0	0	0	0	0	A		
Ge	32	938	2834	0	0	0	0	0	A	19C1-016	AM#2
Sr	38	769	1382	0	(1)	0	0	(1)	B		
Y	39	1522	3338	0	0	(1)	0	(1)	B		
Zr	40	1855	4409	0	0	0	0	0	A		VIM#1
Nb	41	2469	4744	(1)	0	0	0	(1)	B	19C1-015	
Ru	44	2334	4150	(1)	0	0	0	(1)	B		AM#2
Rh	45	1963	3697	0	0	0	0	0	A		
Pd	46	1555	2964	0	0	0	0	0	A	19C1-014	
Ag	47	962	2163	0	0	(1)	0	(1)	B		
In	49	157	2073	0	0	0	0	0	A		
Sn	50	232	2603	0	0	0	0	0	A		
Ba	56	727	1898	0	(1)	0	0	(1)	B		
La	57	918	3457	0	0	(1)	0	(1)	B		
Ce	58	798	3426	0	0	(1)	0	(1)	B	19C1-016	AM#1
Pr	59	931	3512	0	0	(1)	0	(1)	B		
Nd	60	1021	3068	0	0	(1)	0	(1)	B		
Tb	65	1356	3223	0	0	(1)	0	(1)	B	19C1-010	AM#1
Ho	67	1474	2695	0	0	(1)	0	(1)	B		
Er	68	1529	2863	0	0	(1)	0	(1)	B		
Lu	71	1663	3395	0	0	(1)	0	(1)	B		
Hf	72	2231	4603	(1)	0	0	0	(1)	B		AM#1
Ta	73	3020	5458	(1)	0	0	0	(1)	B	19C1-016	AM#1
W	74	3422	5555	(1)	0	0	0	(1)	B	19C1-015	
Re	75	3186	5596	(1)	0	0	0	(1)	B		
Os	76	3033	5012	(1)	0	0	0	(1)	B		
Ir	77	2447	4428	(1)	0	0	0	(1)	B	19C1-015	
Pt	78	1769	3827	0	0	0	0	0	A		
Au	79	1064	2857	0	0	0	0	0	A	19C1-010	VIM#1
Tl	81	304	1473	0	(1)	0	0	(1)	B		
Bi	83	271	1564	0	(1)	0	0	(1)	B		
Th	90	1755	4788	0	0	(1)	0	(1)	B		
Pa	91	1572		0	0	0	0	0	A		

Table 3.3. Predicted second-phase segregation for the chosen taggant elements.

Taggant Element	Predicted Second Phase
Al, Mn, Co, Ni, Ge, Pd, W, Au	Intermetallic
Sc, Ce, Tb	Rare-earth oxide
Ti, Nb, Ta, W	Carbide, nitride, and/or oxide
V	Incorporate into uranium carbide (UC)

3.3. Experimental approach

3.3.1. Casting and sampling

All materials were made using depleted uranium (DU) metal. The nominal carbon level was 245 wppm; total other impurities 750 wppm maximum. They were made by vacuum induction melting (VIM), a common technique used to cast uranium. The baseline alloy process flowsheet is shown in Figure 3.1.

Table 3.4 lists all 18 alloys produced throughout this 3-year study. The baseline alloys (~16 kg) were the first four plates produced. One of the baseline alloys, 19C1-016, reacted with the crucible during VIM casting and was only analyzed for chemistry. The other three successful baseline alloys were combined with one another to produce three mixed alloys while one of them was combined with unalloyed DU to produce the one dilution alloy (all ~5 kg). Finally, the three successful baseline alloys were combined to produce the alloy that was used throughout the recycling study, whose casting mass ranged from 17 kg (1st melt) to 12 kg (final, 10th melt).

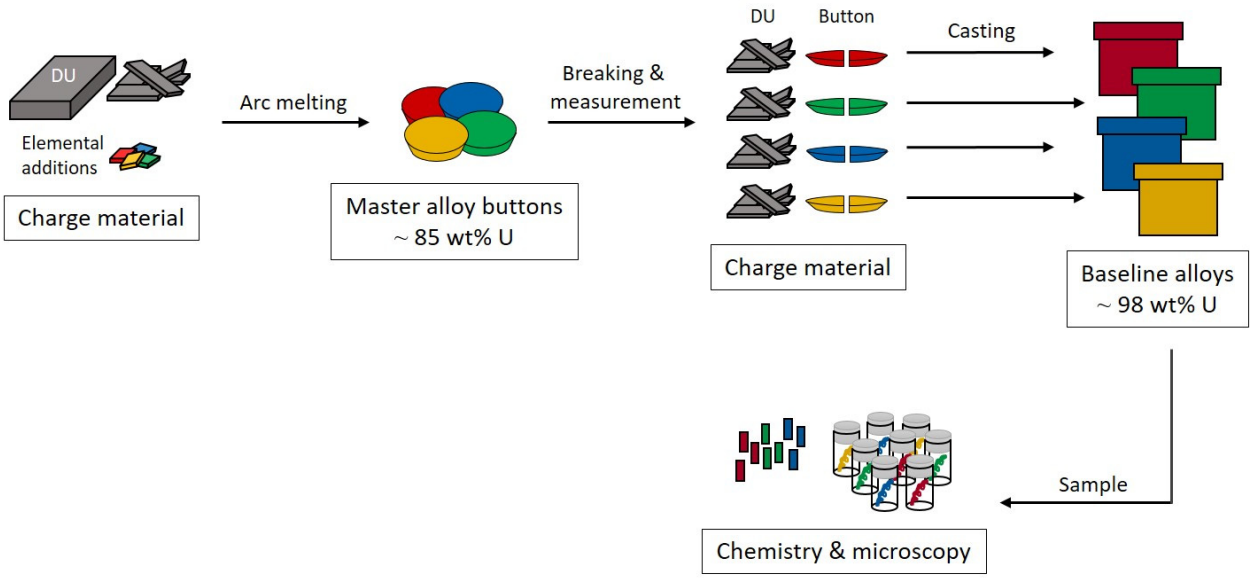

Figure 3.1. Schematic of the processing of the baseline alloys.

Table 3.4. An overview of the 18 uranium alloy castings processed throughout this study.

Group	Casting ID	Taggant Elements Included
Baseline alloys	19C1-010	Ti, Mn, Tb, Au
	19C1-014	Al, Sc, V, Pd
	19C1-015	Co, Nb, W, Ir
	19C1-016*	Ni, Ge, Ce, Ta
Mixed alloys	20C1-076	Al, Sc, V, Co, Nb, Pd, W, Ir
	20C1-077	Al, Sc, Ti, V, Mn, Pd, Tb, Au
	20C1-078	Ti, Mn, Co, Nb, W, Ir, Au
Dilution alloy	20C1-080	Co, Nb, W, Ir
Recycling study	21C1-105	Al, Sc, Ti, V, Mn, Co, Nb, Pd, Tb, W, Ir, Au
	21C1-107	
	21C1-109	
	21C1-111	
	21C1-112	
	21C1-113	
	21C1-114	
	21C1-115	
	21C1-116	
	21C1-118	

*19C1-016 reacted in the crucible; results from this alloy are questionable. Due to resource limitations, it was not studied or used further.

3.3.2. Bulk chemical analysis

The taggant elements in all 18 castings were measured via inductively coupled plasma-mass spectroscopy (ICP-MS) at two different LANL laboratories. Carbon analysis was preformed using a LECO CS844 carbon/sulfur analyzer. Drill turnings from various locations in each plate (typically hot top, middle, and bottom) were analyzed. It was gratifying to learn that most elements did not preferentially segregate to the top or bottom of the plate: the plates were reasonably chemically homogeneous in the as-cast state. Any time one alloys a material (uranium or otherwise), segregation (on length scales too long to be homogenized out – that is, “heat treated” away) is always a concern; hence, this outcome is very encouraging.

3.3.3. Microscopy

Various samples from the baseline alloys and mixed/dilution alloys were metallographically mounted, polished, and examined via light optical microscopy (LOM) and scanning electron microscopy (SEM). Two different SEMs were utilized: an Inspect SEM and a Helios G4 UXE Plasma FIB/SEM. Representative inclusions were analyzed by energy dispersive X-ray spectroscopy (EDS) to determine chemical makeup. EDS has a spatial resolution of about 1-2 microns, which means at best one can qualitatively identify the major elements given the ~1 micron particle sizes in this project; quantitative analysis would require transmission electron microscopy (TEM) coupled with EDS, which was beyond the scope of this project but which might be done in the future.

3.4. Experimental outcomes

3.4.1. Baseline alloys

3 of the 4 baseline alloys were successfully cast. Casting 19C1-016, containing Ni, Ge, Ce, Ta showed an unexpected reaction in the crucible, making it uncertain how much of the tagging elements ended up in the casting. For this reason, it was not studied further, and these 4 elements are grayed out in Table 3.1.

The other 12 elements ended up in their respective baseline castings in varying degrees ranging from ~5 to ~95%, as indicated by the color in Table 3.1 for chemical tagging. The microscopy results allowed a similar assessment to be made of second phase tagging.

The baseline results are not presented here in the interest of brevity. Many of the same themes emerged from the mix, dilution, and recycle results that will now be described with some example outcomes.

3.4.2. Mixed/dilution alloys

The next step in the bulk tagging investigation was to mix and dilute the baseline alloys with the goal of retaining the taggant ratio through another round of processing. Among a possible ten dilution and mixture combinations of the baseline alloys, four were chosen to move forward. Those combinations are shown in Figure 3.2. This resulted in three mixtures from the three successful baseline alloys in approximately a 1:1 ratio and one dilution alloy, a baseline alloy mixed with unalloyed DU in approximately a 1:1 ratio. The alloying elements are expected to become half of their initial values. So, if starting from a nominal 0.5 wt% in the baseline alloy, they will end up at 0.25 wt% in the mixed/dilution alloy.

Figure 3.3 shows the workflow for this part of the study**.** The baseline alloys were split and set aside for casting. The mixed/dilution alloys were cast in a VIM furnace resulting in four plates, similar to the baseline alloys. The plates were then sectioned for metallography, and machine turnings were taken for chemical analysis. Chemical samples were taken from two locations per casting, the middle and the top of the plate. The samples were also analyzed at two different LANL laboratories, same as the baseline alloys.

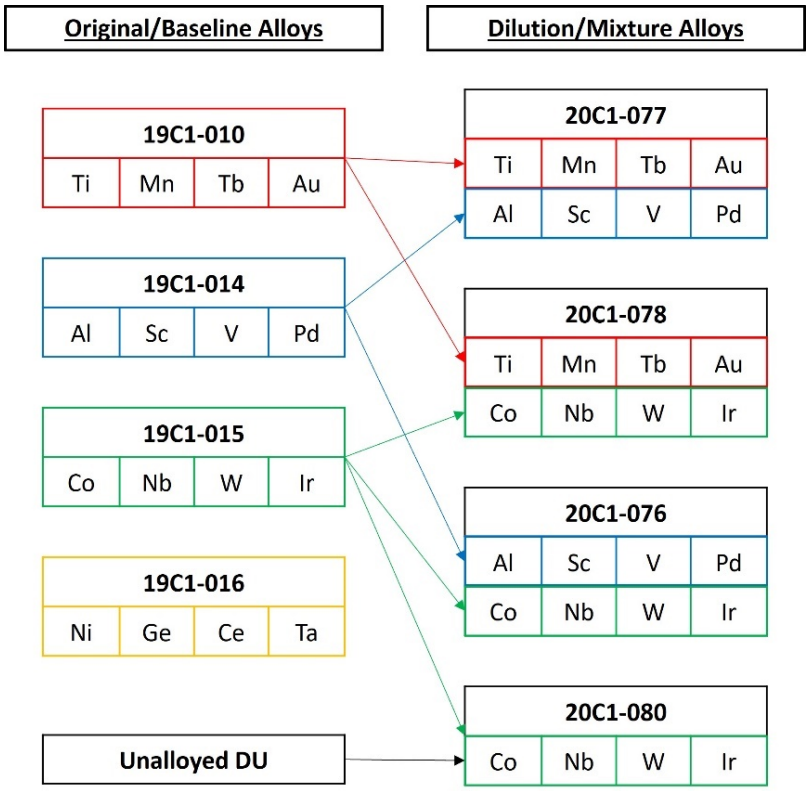

Figure 3.2. Schematic detailing the chosen dilution and mixtures of the original baseline alloys.

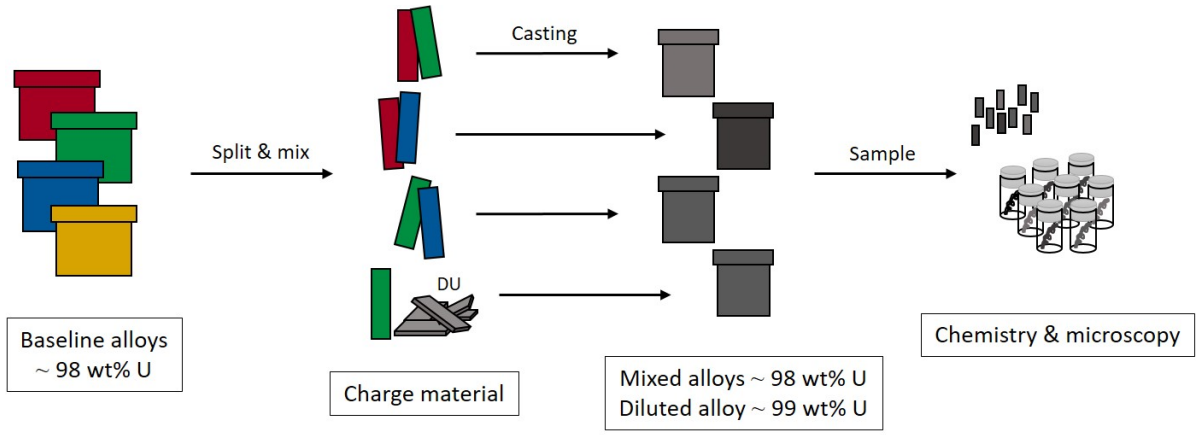

Figure 3.3. Schematic showing the processing of the mixed/diluted alloys.

One of the mix alloys will be used to demonstrate the type of results obtained in this study, 20C1-076. This casting combined two baseline alloys in nearly equal proportions and has 8 intentional tagging elements total: Al, Sc, V, Pd, Co, Nb, W, and Ir.

Chemistry results are plotted in Figure 3.4. The top plot displays absolute weight % values of the calculated and measured concentration of each taggant element along with carbon (a typical impurity in all uranium grades). Measured concentration values from the baseline alloys along with charge weight was used to calculate the expected chemistries for the four mixed/dilution alloys. The bottom plot normalizes the measured values with the calculated values to show what percentage of the taggant element made it into the casting.

There are three items of interest that can be read off this graph:

1. **manufacturability** – as measured by how much of each element made it into the casting,
2. **chemical homogeneity** of the material – the similarity of chemistry measured from the top vs. mid-plate vs. bottom-of-casting, and
3. **detectability** – replicability of analytical Lab A vs. analytical Lab B results

For manufacturability, Al, V, Co, Nb, Pd made it into the mixed alloys at the expected normalized level; of these, not as much Pd made it into the parent baseline alloy in absolute (wt.% value) terms; the same held true of W. Moreover, very little Sc made it into the mixed alloy (~10% of calculated), even accounting for the low level from the parent baseline alloy. (A similar issue was encountered with the element Tb in other alloys not shown here.) Although such deficits can potentially be offset by a deliberate excess being added in baseline alloy creation in future studies, the origin of the behavior of Sc, Pd, and W is yet known and needs further study before it can be considered a suitable chemical taggant.

For chemical homogeneity, there was no significant difference in measurements from the different locations in each alloy, so segregation in the final product is not a concern with the specific elements and foundry practice employed here. Since each of the taggant elements were already well mixed in the charge material, the mixed/dilution alloy results should give a better indication as to whether or not an element will make it through processing and into the final part.

For detectability, 6 elements in this particular mix casting – Al, Sc, V, Co, Nb, Pd – turned out well. By contrast, W and Ir had noticeable differences in each of the three mixed/dilution alloys in they were present, including this one. This raises concerns for these two elements as chemical taggants. If the measurements are not repeatable across laboratories, the elements are not suitable as chemical taggants.

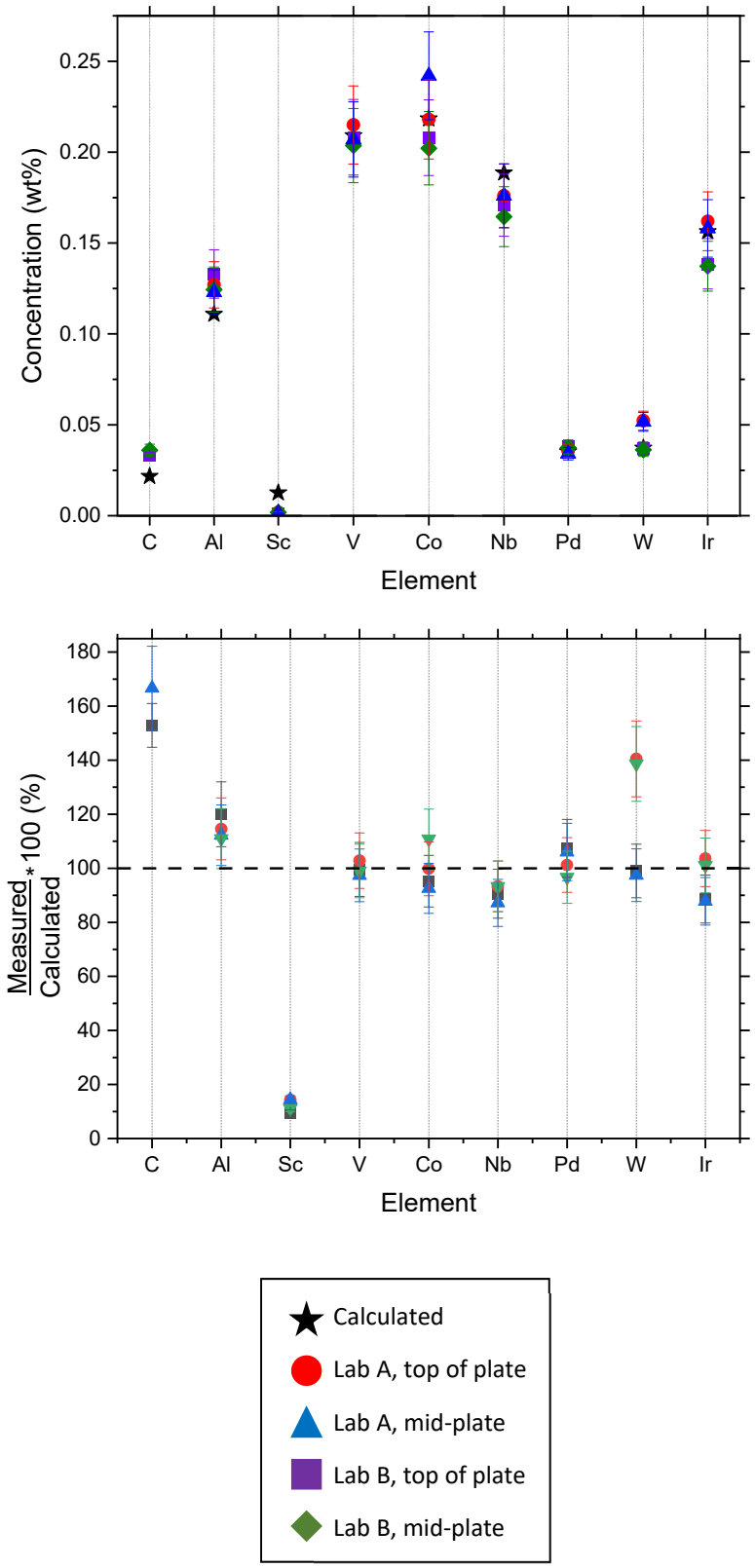

Figure 3.4. Chemical analysis results for carbon and the 8 intentional tagging elements in mix alloy 20C1-076.

Moving to an evaluation of **second phase tagging**, the microscopy (SEM-EDS) results from the same mix alloy 20C1-076 are shown in Figure 3.5.

From a **manufacturability and detectability** point of view, 7 of the 8 elements (all except W) were positively identified in one or more particle shapes. SEM-EDS was unable to determine the crystal structure of the phases, so definitive assignments of each element to specific phases could not be done. But using the distinct shapes of particles along with qualitative information about the presence of carbon (pointing to a carbide phase) and oxygen (pointing to an oxide phase), or their absence (pointing to an intermetallic phase), some inferences could be drawn about how the elements met their expectations going into this study.

As expected, various intermetallic phases were found. One phase throughout the plate contained Al, Co, and Ir. Another intermetallic phase present were in elongated particles that contained Nb, Al, and V. V was expected to incorporate into uranium carbides while Nb was expected to form its own carbide, as it did in the baseline alloy. Some of these elongated particles did contain Pd as well (though this is not indicated in the figures shown here). One other intermetallic was the Co-containing phase, likely U_6Co, which was seen in the baseline alloy. It was outlined with uranium carbide along with an oxide in some locations. Sc formed an oxide phase as anticipated. W, however, was not found.

The overall observations of particle shapes and compositions carried well from the baseline alloys into the mix and dilution alloys, almost as if the mixture was a simple combination of the phases in parent materials. This was not true for all the phases, and there were nuances of composition or morphology that have yet to be more thoroughly explored. It should also be mentioned that simplicity of particle morphology from parent to product not a requirement for good manufacturability, but all the same makes characterization easier than it would be otherwise.

From a **chemical homogeneity** point of view, three samples taken from the top, middle, and bottom of each of the mixed/dilution alloys were examined via LOM and SEM-EDS. There was no significant difference between the locations in each plate in either microstructure or qualitative chemistry of the phases, indicating good homogeneity, which is consistent with the chemical analysis results.

The outcomes for all the elements are summarized in Table 3.1.

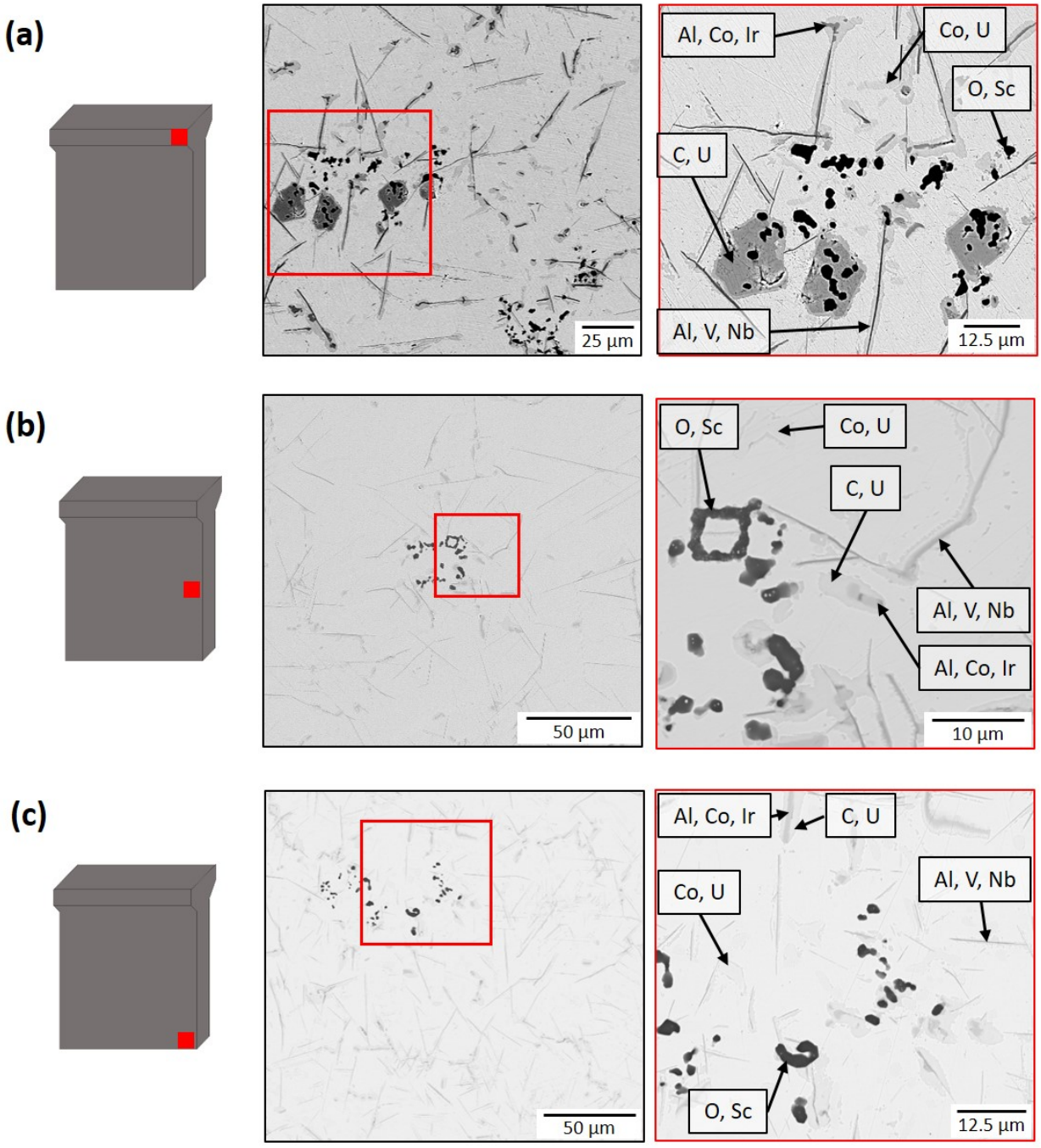

Figure 3.5. Representative BSE-SEM images taken from the (a) hot top, (b) middle, and (c) bottom of mix casting 20C1-076 with intentional tagging elements: Al, Sc, V, Pd, Co, Nb, W, Ir. Inset in low magnification images on left are shown in the higher magnification images on the right. Intermetallic phases of various chemistries and Sc-containing oxides are found throughout the plate. W was unable to be located in any of the second phases via SEM.

3.4.3. Recycling study

One important characteristic of a good elemental taggant in bulk uranium is that it will stick around through further material processing. To determine which of the chosen elements in this study would fill that criteria, a recycling study was designed to see if the taggants were still detectable through ICP-MS after being melted and cast multiple times. A schematic of the workflow is shown in Figure 3.6. The same material would be cast, sampled, and split to go through the process once again with no new material introduced throughout the study.

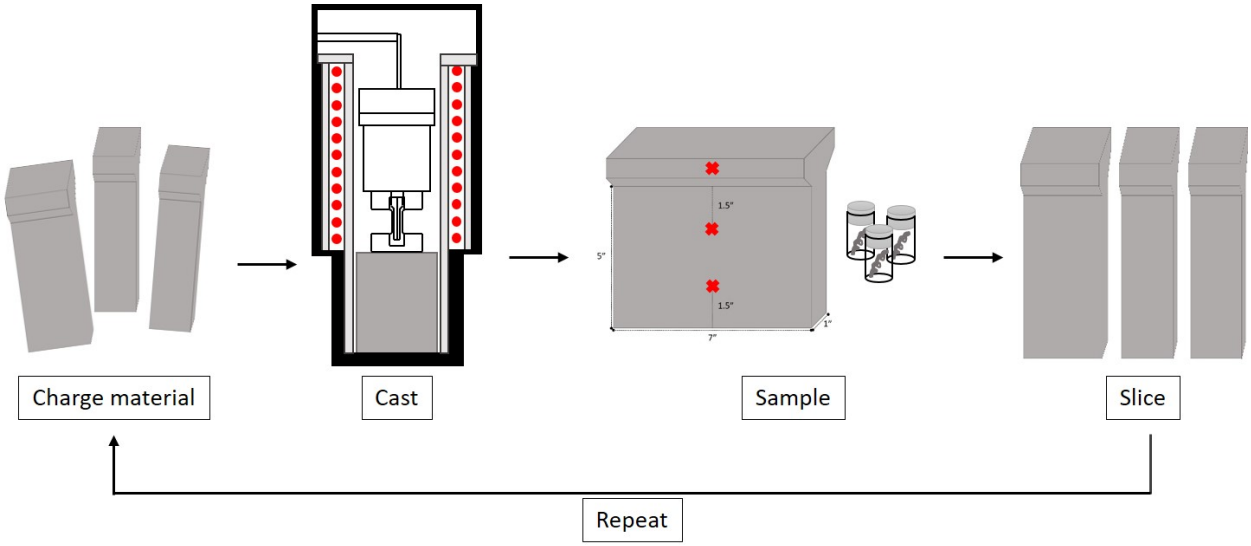

Figure 3.6. Schematic of the workflow for the recycling study. The 3 successful baseline alloys were mixed together, giving 12 intentional tagging elements.

The initial starting charge was a mix of the three successful baseline alloys: 4737 g from 19C1-010, 7751 g from 19C1-014, and 5489 g from 19C1-015. These three alloys were cast into a 5” tall, 7” wide, and 1” thick plate. The as-cast plate was then sliced on a bandsaw to be used as charge material for the next casting. This was repeated for a total of ten castings. All of the casting yields were above 96.90%, indicative of a successful campaign. However, recycling does take its toll: 10 meltings (with minimal loss due to chemistry sample extraction) resulted in a cumulative 32% reduction in the amount of material, the majority of the losses going to the crucible skull and the like. Figure 3.7 shows photos of all 10 recycle castings.

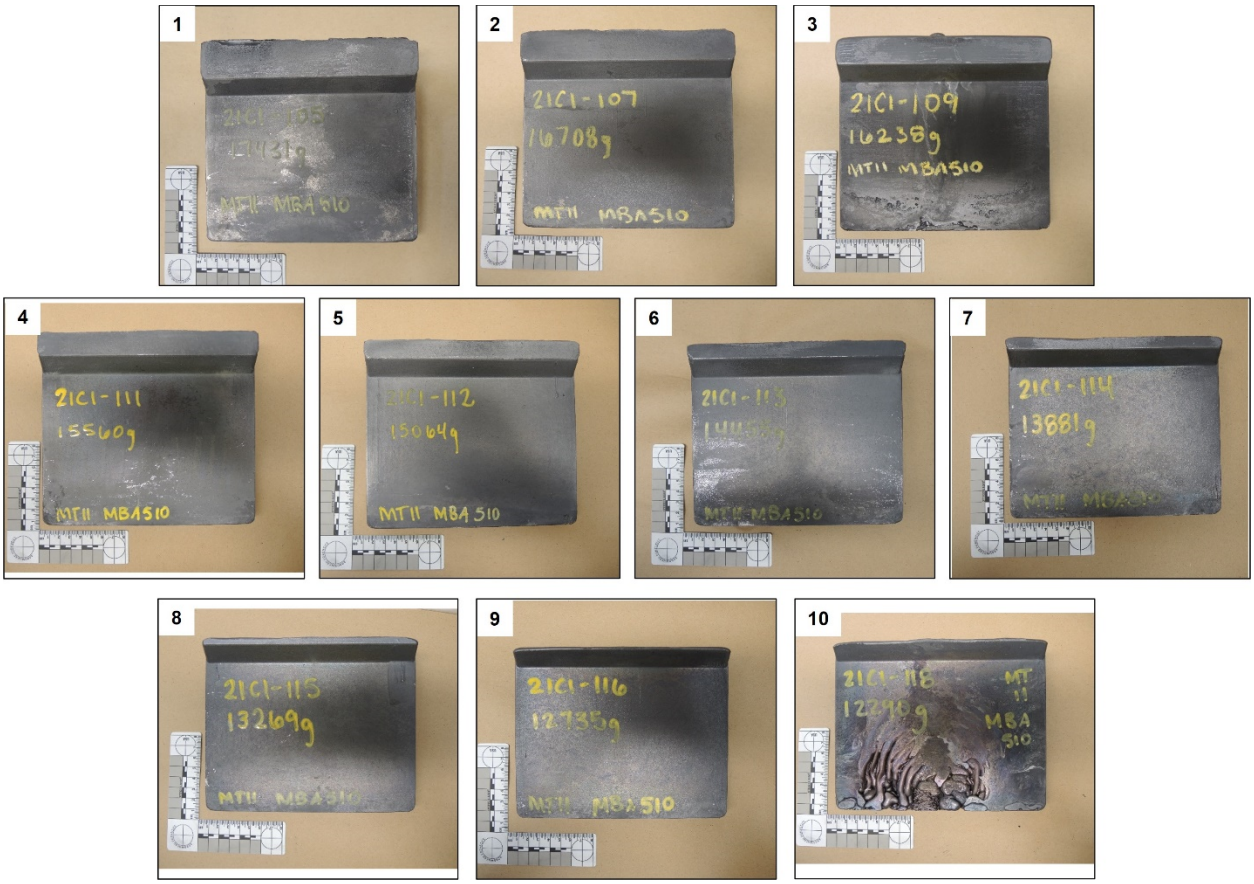

Figure 3.7. Photos of all the as-cast plates from the recycling study. The decreasing charge weights are evident in the decreasing hot top height. Also, the porosity from the mispours on the #3 (21C1-109), and the #10 (21C1-118), castings are visible. This should not impact the chemistry results or the compositions of the successor castings.

No microscopy was done, so only the chemical analysis results are available, and are now summarized. Only one of the 12 elements (Tb) fell out of detection even after 10 meltings, though Sc also posed challenges. Nb did not appear to decrease across ten castings, but it did measure lower than expected. Since this was not an issue in the mixed/dilution castings, more time should be spent determining what occurred before it is ruled in or out as a chemical taggant. For the various reasons explained above, Al, Ti, Pd, W, Ir, and Au would also need to be studied more before a final decision was made. Mn could be experiencing a slight decrease over the ten castings, but more cycles would be needed to determine if this trend was real. V and Co behaved the best, making them ideal candidates for chemical tagging.

3.5. Recommendations for follow-on work

In no particular order, the following are logical next steps in advancing bulk tagging.

3.5.1. Controlling uranium-carbide behavior in liquid uranium in metal fuels

Uranium carbide particles are ubiquitous in nearly all uranium metal applications due to the highly favorable energetics and abundance of carbon sources during processing. While not particularly deleterious at low concentration or small sizes (such as the materials in this study), all metallurgical development efforts whether production, testing, or research - including tagging - must contend with UC formation and any impacts on properties. For example, carbides can float out and in the process take out some of the other tagging elements during manufacture, frustrating efforts to tag thoroughly. Experts must repeatedly address the specifics of inclusion development in uranium products and yet there is a lack of a useful model framework specific to UC phase development with which to interpret, prevent, or respond to issues arising from their presence. Data from a systematic study would benefit process development (especially scale-up) and production control of metallic fuel forms. It initially benefits fuel manufacturers but also helps build a library of tagging signatures for the forensics labs. Although this mainly is geared toward bulk tagging, such research could also inform some surface tagging scenarios.

3.5.2. In-depth crystallographic and chemical characterization of second-phase particles

The SEM-EDS characterization approach was good at identifying *qualitative* patterns of particle shapes, distributions, particle chemistries (i.e., which elements are included, above the detectability limit). The fact that these particle attributes carried through from the baseline into the mix and dilution alloys is gratifying, and makes forensics analysis somewhat easier, However, the scientific closure of the mass balance in the microstructure (i.e., knowledge of the fate of every single element, both intentional tag and impurity alike) could not be done because neither the crystal structure nor the *quantitative* chemical composition of the particles could be determined, given the typical ~0.1-10 micron length scales. Moreover, having 6-14 elements (U, C, and 4-12 tagging species) in the materials in this study prevented confident extrapolation of phase diagram information (crystal structures, compositions, and amounts) based on binary pairs of elements, as higher-order interactions may dominate. Transmission electron microscopy (TEM) studies are recommended to fill this gap, as it provides localized, nm-scale crystallography and chemistry data. Although TEM is not recommended for routine manufacturing process qualification and forensics, it could have a niche role: at least at this stage of bulk tagging technology development, TEM could be is important to provide scientific insight into the lifecycle of tagging elements as they are imparted and altered in the tagged material.

3.5.3. Extension of the recycling study

The recycling study can be continued beyond the 10 melting and casting steps done so far. One might envision going to 20, 30, or even 40 recycles. This will bring out the trends of elemental fates even better, for example manganese that showed a marginal drop after 10 steps but would become more obvious after more steps (assuming the downward trend continued). In addition, this material can also be cut up and used in later studies of dilution, replicability of chemical analysis with additional laboratories, etc. Also, SEM-EDS can be done on the 10th recycle of the material made in this study and later recycling points as well.

3.5.4. Metals chemical analysis of arc melted materials from the previous study

Resource limitations in the previous study prevented metals chemical analysis from being done on the arc-melted materials (though C, N, O, and S analyses were done, as was LOM and SEM-EDS microscopy). Nominal wt.% of the two alloys are:

- **AM#1: U-0.05C-0.1Ce-0.1Tb-0.1Hf-0.1Ta** (all elements expected to form CNO phases)
- **AM#2: U-0.05Ni-0.07Ge-0.1Ru** (all elements expected to form U-X intermetallics)

The materials are still available and can be chemically analyzed for metals. Both alloys were run in good vs. bad atmospheres and in 3 different as-rolled conditions, and the chemistry gives insights into the fate of the various elements in ideal vs. degraded processing environments. Overall, this will provide added information on the suitability of additional tagging elements (Ru, Hf) and a cross-check on the same tags used in the current study (Ni, Ge, Ce, Tb, Ta, Au).

3.5.5. Continued characterization of VIM materials from the previous study

VIM materials from the previous study are available for more extensive chemical analysis (e.g., round robin), dilution studies, and also fresh characterization. These include (nominal wt.%):

- **VIM#1: DU-0.05C-0.05Ti-0.05V-0.05Mn-0.1Zr-0.1Mo-0.1Au** (castings 09K-573 = good atmosphere, 09K-577 = bad atmosphere; microscopy and chemical analysis in hand)
- **VIM#1b: DU-0.15C-0.15Ti-0.15V-0.15Mn-0.3Zr-0.3Mo-0.3Au** (casting 09K-568 = good atmosphere; 3 times the concentration of VIM#1; never characterized)
- **VIM#1c: DU-0.025C-0.025Ti-0.025V-0.025Mn-0.05Zr-0.05Mo-0.05Au** (casting 09K-569 = good atmosphere; 0.5 times the concentration of VIM#1; never characterized)

3.5.6. Heat treatment to reveal second phases more obviously and track their fate in thermomechanical processing and reactor thermal environments.

Solutionizing-quench-and-aging heat treatments (involving gamma-direct-to-alpha or beta-to-alpha transformations of the uranium-rich matrix phase) have the possibility of dissolving some or all of the second phase particles present in the as-cast condition and reprecipitating them in localized regions that make the particles easier to find. This was demonstrated in the VIM#1 alloy that was aged at 625ºC in the previous study, which generated colonies containing precipitates that were distinctive-looking by LOM. This needs to be followed up with additional characterization and also applied to the other materials in the previous or current studies, and the processing space expanded. Heat treatments like these potentially offers a method for more rapid identification of discreet second-phase tags, or at least a pointer on where in the sample to do more intensive characterization. Depending on the phase diagram of the elements in question, this might be a way of distinguishing carbide-oxide-nitride phases from intermetallic phases, based on differential solubilities in the beta (tetragonal) and gamma (BCC)-uranium phases vs. the room-temperature stable alpha (orthorhombic) phase.

A related study would be the evolution to larger sizes and different shapes of tagging particles as a function of prolonged annealing (classical coarsening) and/or thermo-mechanical processing in high-alpha (450-600ºC) or gamma (800-1000 ºC) regions. In addition to providing basic scientific information useful for some manufacturing routes, such data on microstructural stability upon long-term annealing and thermal cycling is important for reactor applications.

3.5.7. Manufacture of DU-based fuel mockup at lower, realistic tag concentrations

A point design might involve downselecting 4-8 elements, with input from reactor and other stakeholders, and create a DU mockup of a tagged fuel composition that would be plausible for reactor use. This would involve lower concentrations of the elements, say <0.1 wt.%. The melting, casting, and detection methods would all be similar. Thermo-mechanical processing steps such as rolling to plate could also be added to the process flowsheet.

ACKNOWLEDGEMENTS

This work was funded by U.S. Department of Energy Office of Nonproliferation Research & Development (NA-22). Cheryl Hawk, Andrew Duffield, Brett Preston and Stephen Wiest are acknowledged for their assistance with brainstorming and technical support for the surface tagging efforts. The entire foundry and solidification science team of Sigma Division is thanked for their help with the casting of all 18 bulk tagging alloys, especially Hunter Swenson, Ray Sandoval, Kaegan Schultz, Garry Sandoval, Anthony Florez, Eunice Solis, and Casey Shoemaker. We acknowledge Kevin Bohn for microscopy specimen preparation and the bulk chemical analysis work of Becky Chamberlin, Kevin Boland, Gabrielle Kral, Conor Emberley, Michael Rearick and Kevin Kuhn. Tim Baker and Jessica Lopez helped with the idea development in the early stages of this project.

REFERENCES

2013hac R.E. Hackenberg, “Forensics and Safeguards of Uranium Metal Weaponization: Final Project Report,” report LA-CP-13-00583, Los Alamos National Laboratory, Los Alamos, NM (9 May 2013). From NA-22 project LA09-WPT260-PD04. OUO.

2019hac R.E. Hackenberg, T.J. Baker, A.N. Black, J.S. Carpenter, J.C. Cooley, S.D. Imhoff, J.J. Lopez, K.E. Luitjohan, E.P. Luther, C.J. Montgomery, J.A. Stull, and E.L. Tegtmeier “Intentional Uranium Tagging for Material Provenance and Pathway Forensics (LA19-Intentional-Forensics-NDD3Bb): Annual Report for FY19,” Los Alamos National Laboratory, report LA-CP-19-20691 (October 2019), 57 pp. OUO.

2020hac R.E. Hackenberg, A.N. Black, S.D. Imhoff, K.E. Luitjohan, C.J. Montgomery, L.B. O’Brien, and E.L. Tegtmeier “Intentional Uranium Tagging for Material Provenance and Pathway Forensics (LA19-Intentional-Forensics-NDD3Bb): Annual Report for FY20,” Los Alamos National Laboratory, report LA-CP-20-20637 (October 2020), 40 pp. OUO.

2021hac R.E. Hackenberg, K.E. Luitjohan, L.B. O’Brien, A.N. Black, R.A. Bloom, S.D. Imhoff, C.J. Montgomery, E.L. Tegtmeier, W.P. Winter III, “Intentional Uranium Tagging for Material Provenance and Pathway Forensics (LA19-Intentional-Forensics-NDD3Bb): Annual Report for FY21,” report LA-UR-21-32430, Los Alamos National Laboratory (December 2021), 80 pp. Unclassified and publically released.

2021blo R. Bloom, “Photoluminescence in Tagging: A Glowing Review,” report LA-UR-21-31632, Los Alamos National Laboratory (November 2021), 19 pp. Unclassified and publically released. doi.org/10.2172/1833235